Supporting Information

Efficient Singlet Fission in Rubicene Null Aggregates

Xiaomei Shi,[1]* Xinyu Chen,[2] Yu Huang,[3] Zuyuan Liu,[2] Bo Zhao,[2] Lingpeng Yan,[2] Teng-Shuo Zhang[3]* Hongbing Fu,[4] and Long Wang[2]*

[1]Department of Biochemistry and Molecular Biology, Shanxi Medical University, Taiyuan 030001, P. R. China

[2]Key Laboratory of Interface Science and Engineering in Advanced Materials, Ministry of Education, Taiyuan University of Technology, Taiyuan 030024, P. R. China

[3]College of Chemical Engineering, Zhejiang University of Technology, Hangzhou, Zhejiang 310014, P. R. China

[4]Beijing Key Laboratory for Optical Materials and Photonic Devices, Department of Chemistry, Capital Normal University, Beijing 100048, P. R. China

Corresponding Authors:

*X. M. S., email: shxm@sxmu.edu.cn

*T.-S. Z., email: zhangts@zjut.edu.cn

*L. W., email: wanglong@tyut.edu.cn

Table of Contents

1. Materials and Methods.

All solvents and reagents of the best grade available were purchased from commercial suppliers and used without further purification. Single crystals were grown by the vapor diffusion of petroleum ether (poor solvent) into a dichloromethane solution (good solvent). Neat film samples were prepared by vapor deposition method on a sapphire substrate at a rate of 0.3 Å/s under a vacuum of 10^{-5} mbar. X-ray diffraction (XRD) was carried out in the reflection mode at room temperature using a 2 kW Rigaku XRD system (Rigaku, Japan).

UV-visible absorption and photoluminescence (PL) spectra were measured on Shimadzu UV-3600 and Hitachi F-4500 spectrophotometers, respectively. Transient PL attenuation tests were performed by the Edinburgh FLS980 spectrometer equipped with an EPL-515 picosecond pulsed diode laser. Femtosecond transient absorption (fs-TA) and nanosecond transient absorption (ns-TA) spectroscopy measurements were all performed using previously described instruments and experimental conditions.[1-3] Analysis of the kinetic traces derived from time-resolved spectra was performed using nonlinear least-square fitting to a general sum-of-exponentials function after deconvolution of instrument response function. All the spectroscopic measurements were carried out at room temperature.

2. Synthetic Routes.

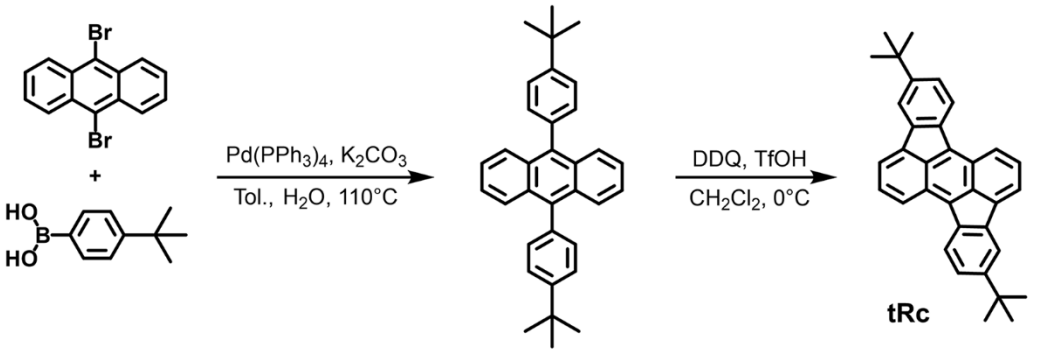

Scheme S1. The synthetic routes of the studied tRc molecule.[4]

Synthesis of Intermediate. A mixture of 9,10-dibromoanthracene (1.0 g, 2.97 mmol), 4-*tert*-butyl phenylboronic acid (1.32 g, 7.44 mmol), potassium carbonate (K_2CO_3, 2.06 g, 8.91 mmol), and tetrakis(triphenylphosphine) palladium ($Pd(PPh_3)_4$, 0.17 g, 0.15 mmol) was dissolved in toluene (Tol., 15 mL) and H_2O (5 mL). The mixed solution was kept stirring under nitrogen atmosphere and then 100 ℃ for 10 h. After cooling to room temperature, the whole was added to H_2O (100 mL). The organic materials were extracted with CH_2Cl_2 (3 × 100 mL). The combined organic layers were dried ($MgSO_4$) and evaporated. The crude product was purified by column chromatography (petroleum ether/dichloromethane, v/v = 5:1) to obtain the intermediate 9,10-bis(4-(tert-butyl) phenyl)anthracene as light yellow solid (0.9 g, yield 70 %).

Synthesis of tRc. Intermediate 9,10-bis(4-(*tert*-butyl) phenyl)anthracene (0.5 g, 1.13 mmol) and 2,3-dichloro-5,6-dicyano-*p*-benzoquinone (DDQ, 0.77 g, 3.39 mmol) were added to anhydrous CH_2Cl_2 (15 mL) was stirred for 10 min in an ice bath at 0 ℃ under nitrogen atmosphere. After the addition of Trifluoromethanesulfonic acid (TfOH, 0.80 mL, 7.51 mmol), the mixture was stirred for 1h at 0 ℃. The reaction mixture was poured into aq $NaHCO_3$ (50 mL) and rinsed with H_2O (50 mL). The organic materials were extracted with CH_2Cl_2 (3 × 50 mL). The combined organic layers were dried ($MgSO_4$) and evaporated. The crude product was purified by column chromatography (petroleum ether/dichloromethane, v/v = 3:1) to obtain the *tert*-butyl rubicene as red solid (0.2 g, yield 40 %). ^{1}H NMR (400 MHz, Dichloromethane-d) δ 8.58 (d, *J* = 8.4 Hz, 2H), 8.24 (d, *J* = 8.0 Hz, 2H), 7.98-8.09 (m, 4H), 7.78 (t, *J* = 7.5 Hz, 2H), 7.47-7.52 (m, 2H), 1.47 (s, 18H).

3. Crystal Structures and Molecular Packing Arrangements

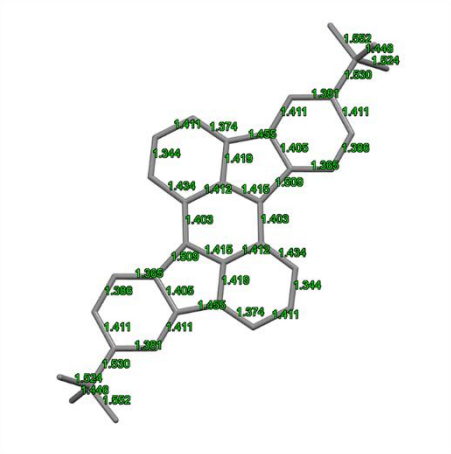

Figure S1. Molecular structure (bond length, unit: Å) in tRc crystal structures.

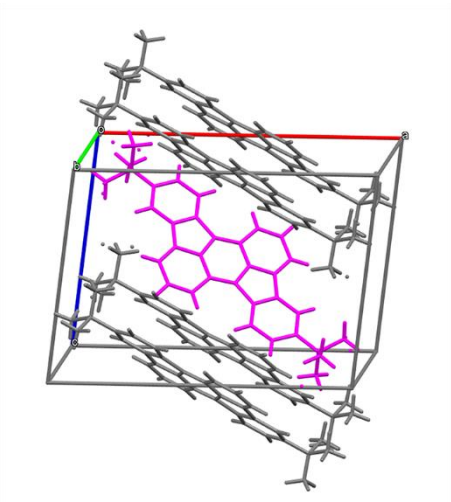

Figure S2. Molecular packing arrangements in tRc crystal cell.

4. Theoretical Calculations.

All the calculations were carried out with the Gaussian 16 program package.[5] The ground state (S_0) geometry was optimized at the B3LYP/6-311G(d) level. The geometries and the excitation energies of the triplet and singlet states were optimized and calculated using density functional theory (DFT) and time dependent density functional theory (TDDFT) methods, respectively. Tamm-Dancoff approximation (TDA) was applied in calculations in consideration of the instability of triplet states.[6]

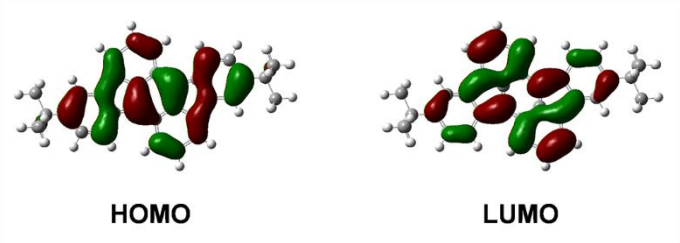

Figure S3. Molecular orbitals of tRc molecule.

Exciton Coupling Calculations. The dimer structures are extracted from the single crystal. Long-range Coulombic coupling (J_{Coul}) is calculated using the point dipole approximation[7,8]:

$$J_{\mathrm{Coul}} = \frac{\mu^2(1-3cos^2\theta)}{4\pi\varepsilon R^3}$$

where μ is the transition dipole moment, θ is the slipping angle, ε is the medium dielectric constant, and R is the interchromophore distance.

Short-range charge transfer (CT) coupling (J_{CT}) can be approximated by[8-10]:

$$J_{\mathrm{CT}} = \frac{-2t_{\mathrm{e}}t_{\mathrm{h}}}{E_{\mathrm{CT}} - E_{\mathrm{S_1}}}$$

where t_e and t_h are the electron and hole transfer integrals between two chromophores, respectively, and E_{CT} and E_{S1} are the energy of the CT state and the first singlet excited state, respectively.[11] Electron-hole analysis was performed via Multiwfn software to determine the CT state.[12]

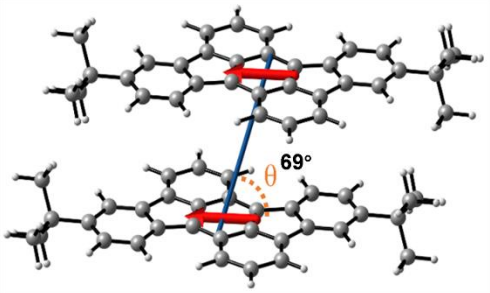

Figure S4. The transition dipole moment of tRc molecule and the relative slip angle between transition dipole moments of adjacent dimer unit from the crystal data.

Table S1. The excited state energies and corresponding parameters for exciton coupling theoretical analysis.

Parameters	Values
μ	1.837×10^{-29} C m
θ	69.3 °
R	6.23 Å
t_e	190.4 cm^{-1}
t_h	400.8 cm^{-1}
E_{CT}	2.19 eV
E_{S1}	2.09 eV
J_{Coul}	391 cm^{-1}
J_{CT}	−195 cm^{-1}

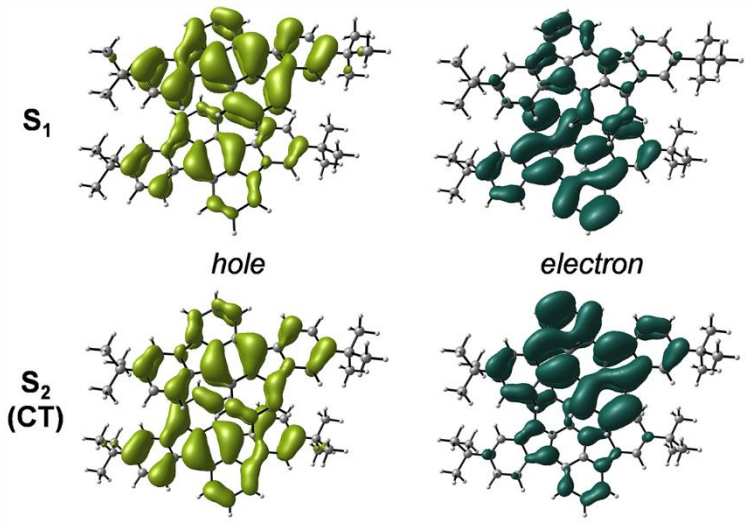

Figure S5. The electronic transition characters of the relevant excited state.

5. Supplementary Data for TA Measurements.

5.1 TA Measurements in Dilute Solution.

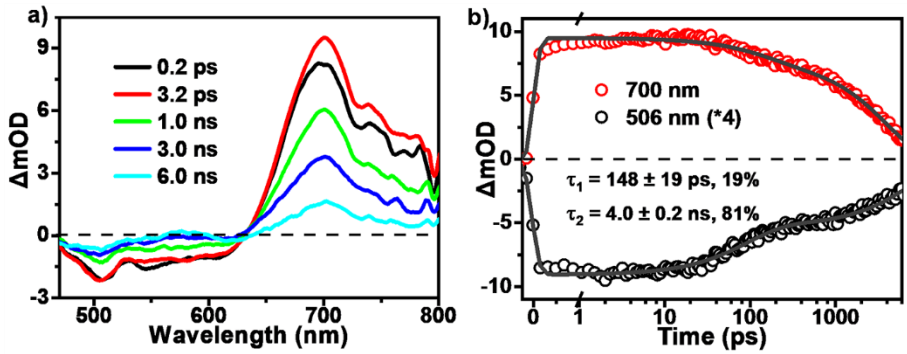

Figure S6. TA measurements in dilute solution of tRc molecule. a) TA spectra and b) selected kinetic decay curves (450 nm-excitation).

5.2 Heat Effect Elimination.

In order to ensure that the observed dynamics in thin films were not or do not include the heat artifacts of excitation laser source, the absorption spectra of thin films on sapphire substrate were measured at different temperatures **(Figure S7)**. The results indicate that absorption line shapes of these thin films show no obvious changes as temperatures elevated from 20 to 100 ℃. Therefore, no noticeable thermal effects are observed in TA measurement for thin films. Then excitation density dependence measurements were also conducted for film tests (**Figure S8**). The samples were subjected to 450 nm excitation at varied fluences. The results show that no significant difference of lifetime is observed between high and low in excitation light fluences, as evidenced by the ESA decay and GSB recovery dynamics, which indicate that the TA dynamics in thin film are free of concentration quenching artifacts, such as singlet-singlet annihilation and heat effect.

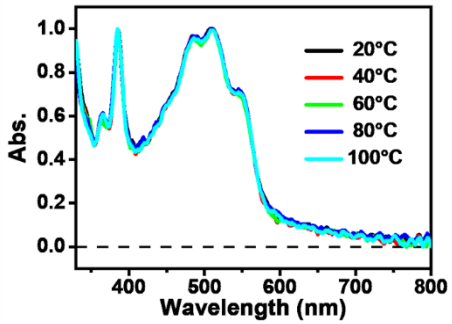

Figure S7. Absorption spectra of tRc thin films at different temperatures on sapphire substrate.

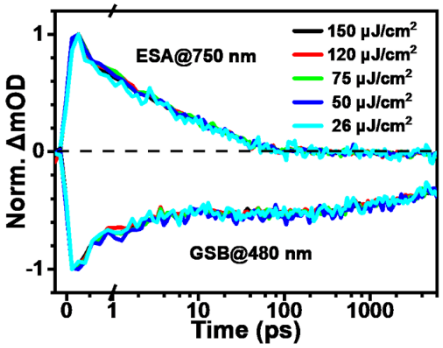

Figure S8. Normalized kinetic profiles for thin film upon excitation at 450 nm with different excitation densities. The results show that the excitation density has little impact on the excited-state dynamics in fs-TA measurement for solid films.

5.3 Triplet Decay Dynamics in Thin Films.

Nanosecond TA (ns-TA) measurements were performed to track the deactivation of the long-lived transient species. The TA signals on a time scale of ns-to-μs recovered back to ground line without further evolution. Given the line shapes of these signals in the ns-TA spectra overlap well with the fs-TA spectral signature, the dominant end species formed upon photo-excitation are undoubtedly individual triplet excitons. The SF-generated triplet excitons

exhibit a characteristic biexponential decay kinetics (**Figure S9)**. These two distinct triplet decay components were then assigned to i) triplet states undergoing *in situ* triplet-triplet annihilation back in the S_0 with $\tau_1 = 219 \pm 12$ ns (63.2%) and ii) triplet states that diffuse before annihilation back in the S_0 with $\tau_2 = 2441 \pm 80$ ns (36.8%), respectively.

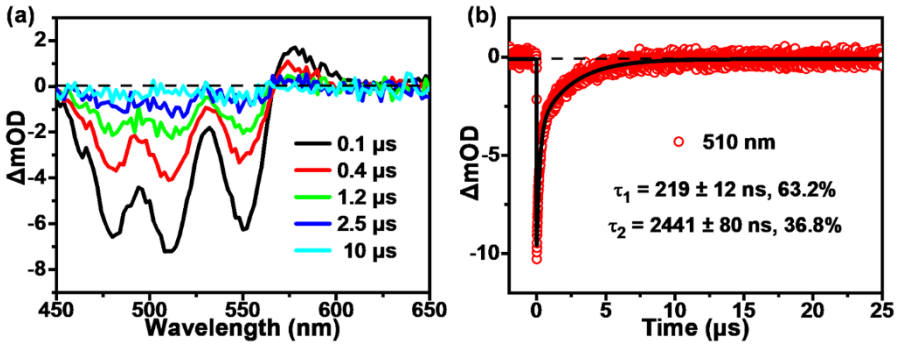

Figure S9. Triplet-state decay dynamics. a) ns-TA spectra and (b) selected kinetic decay curves of tRc films (excited at 532 nm).

5.4 Triplet Yield Determination.

Triplet yield was estimated using singlet depletion method based on quantifying GSB signal in ns-TA data and relating this exciton density to the calculated exciton density due to the laser power, spot size, and the film thickness and absorption.[13] These values were used to calculate an excitation density:

$$\xi = \frac{E \cdot \lambda \cdot K \cdot (1 - 10^{-A})}{l \cdot a}$$

As well as number density:

$$No.Density = \frac{Z}{V}$$

The ratio of which (ξ/No. Density) gives a scaling factor for the ground state absorption spectrum that produces the amount of GSB at t_0 or with 100% triplet yield. We then examine the actual bleach necessary to produce the pure triplet absorption spectrum from the ns-TA spectra and compare this to the calculated bleach. To more strictly quantify this analysis we can focus on a region where the GSB spectrum is strongly featured. As outlined by Carmichael and Hug,[14] addition of the ground state absorption spectrum to the transient trace so as to remove the minimum at this position yields a reasonable triplet-triplet absorption spectrum. These traces then give approximate measure of the GSB addition necessary to obtain a purely triplet-triplet spectrum and, thus, the triplet yield. The amount of GSB necessary to produce a linear trace in this region is used as the yield. The experimental error is derived from these traces as

these errors are found to be greater than the error from measurement uncertainties. As the yield is determined from a 100 ns TA trace, a portion of the triplet population has decayed as a result of triplet-triplet annihilation. To correct for this, the yield is extrapolated to using the triplet annihilation kinetics:

$$TY\% = TY\%_{100\ ns} \cdot \frac{1}{A_1 \cdot e^{-100/\tau_1} + A_2 \cdot e^{-100/\tau_2}}$$

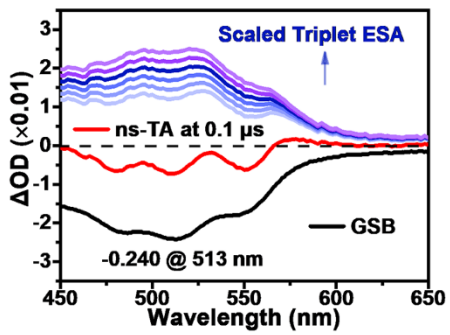

Figure S10. Triplet-triplet absorption spectra. Spectra are created by addition of scaled GSB (black) to the 100 ns-TA spectrum (red).

Table S2. Laser and sample parameters for triplet yield analysis.

Parameters	Values
Original Data	
Excitation Energy (**E**)	0.0016 *J*
Excitation Wavelength (**λ**)	532 *nm*
Constant **K**	$5.034\times10^{15}\ J^{-1}nm^{-1}$
Absorbance at excitation ($\mathbf{A_\lambda}$)	0.100 (532 nm)
Film thickness (**l**)	54 *nm*
Excitation spot size (**a**)	0.785 cm^2
Formula units/cell (**Z**)	2
Unit cell volume (**V**)	1226.7 $Å^3$
Absorbance at triplet ($\mathbf{A_T}$)	0.130 (513 nm)
Triplet annihilation kinetics (amplitudes) $\boldsymbol{\tau_1}$ **(A1)** and $\boldsymbol{\tau_2}$ **(A2)**	219 ns (63.2%) and 2441 ns (36.8%)
Derived Data	
Excitation density (**ξ**)	$2.079\times10^{20}\ cm^{-3}$
No. Density	$1.630\times10^{21}\ cm^{-3}$
Expected bleach	–0.0240
Scaled bleach	–0.0167 (550 nm)
Triplet yield at 100 ns ($\mathbf{TY\%_{100\ ns}}$)	145 ± 30%
Triplet yield (TY%)	192 ± 30%

6. References.

1. Wang, L.; Bai, S.; Wu, Y.; Liu, Y.; Yao, J.; Fu, H., Revealing the Nature of Singlet Fission under the Veil of Internal Conversion. *Angew. Chem. Int. Ed.* **2020**, *59*, 2003-2007.

2. Wang, L.; Lin, L.; Yang, J.; Wu, Y.; Wang, H.; Zhu, J.; Yao, J.; Fu, H., Singlet Fission in a Pyrrole-Fused Cross-Conjugated Skeleton with Adaptive Aromaticity. *J. Am. Chem. Soc.* **2020**, *142*, 10235-10239.

3. Wang, L.; Zhang, T.; Fu, L.; Xie, S.; Wu, Y.; Cui, G.; Fang, W.; Yao, J.; Fu, H., High-Lying 3^1Ag Dark-State-Mediated Singlet Fission. *J. Am. Chem. Soc.* **2021**, *143*, 5691-5697.

4. Kawamura, M.; Tsurumaki, E.; Toyota, S. Facile Synthesis of Rubicenes by Scholl Reaction. *Synthesis* **2018**, *50*, 134-138.

5. Frisch, M. J.; Trucks, G. W.; Schlegel, H. B., et al., Gaussian, Inc., Wallingford CT, Gaussian 16. **2016**.

6. S. Hirata; M. Head-Gordon, Time-dependent Density Functional Theory within the Tamm-Dancoff Approximation. *Chem. Phys. Lett.* **1999**, *314*, 291-299.

7. Kasha, M.; Rawls, H. R.; Ashraf El-Bayoumi, M. The Exciton Model in Molecular Spectroscopy. *Pure. Appl. Chem.* **1965**, *11*, 371-392.

8. Hestand, N. J.; Spano, F. C. Interference between Coulombic and CT-Mediated Couplings in Molecular Aggregates: H- to J Aggregate Transformation in Perylene-Based π-Stacks. *J. Chem. Phys.* **2015**, *143*, 244707.

9. Hestand, N. J.; Spano, F. C. Expanded Theory of H- and J Molecular Aggregates: The Effects of Vibronic Coupling and Intermolecular Charge Transfer. *Chem. Rev.* **2018**, *118*, 7069-7163.

10. Spano, F. C. The Spectral Signatures of Frenkel Polarons in H and J-Aggregates. *Acc. Chem. Res.* **2010**, *43*, 429-439.

11. Brown, J. S. CATNIP, Version 1.4, **2018**, https://github.com/JoshuaSBrown/QC_Tools.

12. Lu, T.; Chen, F. Multiwfn: A Multifunctional Wavefunction Analyzer. *J. Comput. Chem.* **2012**, *33*, 580-592.

13. Margulies, E. A.; Logsdon, J. L.; Miller, C. E.; Ma, L.; Simonoff, E.; Young, R. M.; Schatz, G. C.; Wasielewski, M. R., Direct Observation of a Charge-Transfer State Preceding High-Yield Singlet Fission in Terrylenediimide Thin Films. *J. Am. Chem. Soc.* **2017**, *139*, 663-671.

14. Carmichael, I.; Hug, G. L., Triplet-Triplet Absorption Spectra of Organic Molecules in Condensed Phases. *J. Phys. Chem. Ref. Data* **1986**, *15*, 1-250.

7. Appendix.

Table S3. Crystallographic parameters for crystal.

Compound	tRc
CCDC	2349726
Empirical formula	$C_{34}H_{30}$
Formula weight	438.58
Temperature/K	302.33(10)
Crystal system	monoclinic
Space group	$P2_1/c$
a/Å	16.485(2)
b/Å	6.2347(7)
c/Å	12.1050(18)
α/°	90
β/°	99.627(13)
γ/°	90
Volume/Å^3	1226.7(3)
Z	2
ρ_{calc}g/cm^3	1.187
μ/mm^{-1}	0.502
F(000)	468.0
Crystal size/mm^3	0.13×0.11×0.07
Radiation	Cu Kα (λ = 1.54184)
2Θ range for data collection/°	5.438 to 152.494
Index ranges	$-20 \le h \le 20$, $-3 \le k \le 7$, $-15 \le l \le 14$
Reflections collected	7656
Independent reflections	2415 [R_{int} = 0.0348, R_{sigma} = 0.0410]
Data/restraints/parameters	2415/36/187
Goodness-of-fit on F^2	1.079
Final R indexes [I >=2σ (I)]	R_1 = 0.0798, wR_2 = 0.2448
Final R indexes [all data]	R_1 = 0.10331, wR_2 = 0.2706
Largest diff. peak/hole / e Å^{-3}	0.37/–0.17

NMR and HRMS Spectra.

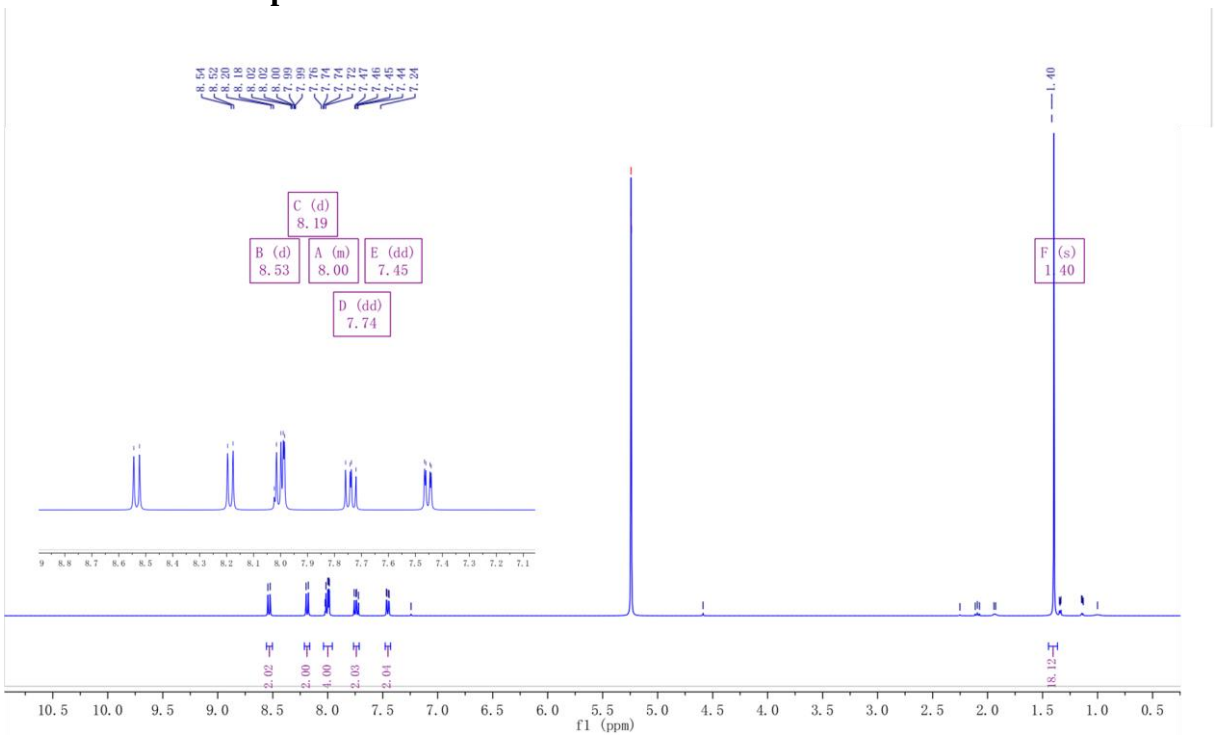

Figure S11. ^{1}H NMR spectra of tRc molecule in CD_2Cl_2.

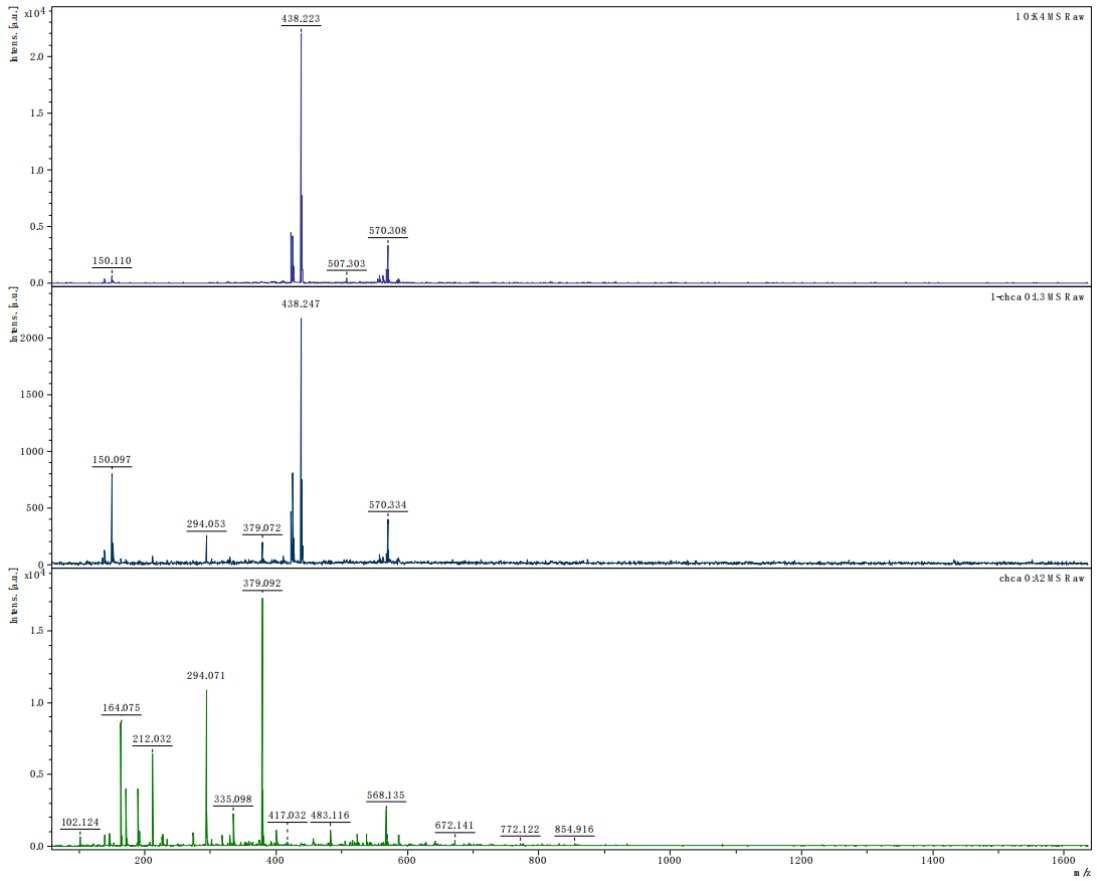

Figure S12. HRMS spectra of tRc molecule.

Optimized Geometries.

S_0 state

Center Number	Atomic Number	Forces (Hartrees/Bohr) X	Y	Z
1	6	-0.000003186	-0.000000931	0.000001328
2	6	-0.000004957	0.000000546	-0.000001475
3	6	-0.000002341	0.000000819	0.000004347
4	6	-0.000002072	-0.000000297	-0.000002939
5	6	0.000003298	0.000000885	0.000001594
6	6	0.000005245	-0.000000560	-0.000001586
7	6	0.000002240	-0.000000873	0.000004437
8	6	0.000001814	0.000000402	-0.000003842
9	6	-0.000009385	-0.000002706	-0.000002276
10	6	-0.000008031	0.000001238	0.000002463
11	6	0.000010882	0.000007838	0.000000405
12	6	0.000004443	-0.000017172	-0.000003167
13	6	-0.000004153	0.000004612	0.000002437
14	6	0.000009109	0.000002850	-0.000002998
15	6	0.000008241	-0.000001330	0.000002170
16	6	-0.000010830	-0.000007898	0.000001263
17	6	-0.000004631	0.000017299	-0.000003267
18	6	0.000004353	-0.000004694	0.000002357
19	6	0.000009015	-0.000004065	-0.000001055
20	6	-0.000009079	0.000004069	-0.000000168
21	6	0.000007677	-0.000000189	0.000000271
22	6	-0.000004980	0.000000788	-0.000000064
23	6	0.000001589	-0.000001079	-0.000000050
24	6	0.000001321	0.000003561	-0.000000019
25	6	-0.000008244	0.000002228	0.000002121
26	6	-0.000002670	-0.000002525	0.000000293
27	6	-0.000001778	-0.000001055	-0.000000353
28	6	0.000008453	-0.000002241	0.000001403
29	6	-0.000001311	-0.000003482	-0.000000009
30	6	0.000001733	0.000001019	-0.000000511
31	6	0.000002610	0.000002515	0.000000115
32	6	-0.000007599	0.000000170	0.000000839

33	6	0.000004986	-0.000000785	-0.000000417
34	6	-0.000001666	0.000001065	0.000000106
35	1	-0.000003263	0.000001000	-0.000000268
36	1	0.000000406	-0.000001395	-0.000000290
37	1	0.000004857	-0.000000284	0.000000896
38	1	-0.000004718	-0.000006198	0.000000427
39	1	-0.000001364	-0.000003983	-0.000000085
40	1	0.000000268	-0.000001237	0.000001234
41	1	-0.000000399	-0.000003748	-0.000000364
42	1	-0.000000288	-0.000001778	-0.000001065
43	1	0.000001004	-0.000004849	-0.000001710
44	1	0.000004521	-0.000001217	-0.000000469
45	1	-0.000000427	0.000001406	-0.000000336
46	1	-0.000006063	0.000000486	0.000001422
47	1	0.000005634	0.000006448	0.000000084
48	1	0.000001527	0.000004055	-0.000000141
49	1	-0.000000263	0.000001126	0.000001338
50	1	0.000000210	0.000003682	-0.000000349
51	1	0.000000303	0.000001886	-0.000000981
52	1	-0.000002027	0.000004621	-0.000001616
53	1	0.000001354	-0.000001418	-0.000000017
54	1	-0.000000001	-0.000004604	0.000001325
55	1	0.000001424	0.000000202	-0.000001753
56	1	-0.000001361	0.000001382	0.000000107
57	1	0.000000125	0.000004550	0.000001878
58	1	-0.000001551	-0.000000125	-0.000002060
59	1	-0.000001133	0.000002184	-0.000000032
60	1	-0.000000984	-0.000001104	-0.000000011
61	1	-0.000001865	-0.000000984	-0.000000299
62	1	0.000001867	0.000000948	-0.000000405
63	1	0.000001120	-0.000002179	-0.000000168
64	1	0.000000990	0.000001102	-0.000000048

T_1 state

Center Number	Atomic Number	Atomic Type	Coordinates (Angstroms) X	Y	Z
1	6	0	-7.541712	1.415044	0.000023

2	6	0	-7.700928	-0.733480	1.261250
3	6	0	-7.700941	-0.733460	-1.261235
4	6	0	-7.109354	-0.061855	0.000010
5	6	0	7.541712	-1.415044	0.000013
6	6	0	7.700928	0.733472	1.261254
7	6	0	7.700940	0.733468	-1.261231
8	6	0	7.109354	0.061854	0.000009
9	6	0	-2.770996	-0.647792	-0.000003
10	6	0	-3.651832	-1.742744	0.000004
11	6	0	-5.021274	-1.523584	0.000007
12	6	0	-5.581317	-0.227785	0.000002
13	6	0	-4.701758	0.868687	-0.000002
14	6	0	2.770996	0.647792	-0.000002
15	6	0	3.651832	1.742744	0.000005
16	6	0	5.021274	1.523584	0.000008
17	6	0	5.581317	0.227785	0.000003
18	6	0	4.701758	-0.868687	-0.000002
19	6	0	-3.329339	0.673856	-0.000005
20	6	0	3.329339	-0.673856	-0.000004
21	6	0	2.222232	-1.636172	-0.000008
22	6	0	2.149994	-3.034117	-0.000011
23	6	0	0.891329	-3.635785	-0.000014
24	6	0	-0.290924	-2.882421	-0.000013
25	6	0	1.341203	0.538514	-0.000005
26	6	0	1.037030	-0.886372	-0.000007
27	6	0	-0.245375	-1.477064	-0.000008
28	6	0	-1.341203	-0.538514	-0.000005
29	6	0	0.290924	2.882421	-0.000012
30	6	0	0.245375	1.477064	-0.000008
31	6	0	-1.037030	0.886372	-0.000008
32	6	0	-2.222232	1.636172	-0.000008
33	6	0	-2.149994	3.034117	-0.000011
34	6	0	-0.891329	3.635785	-0.000014
35	1	0	-7.184374	1.947823	-0.885413
36	1	0	-8.633012	1.480086	0.000026
37	1	0	-7.184371	1.947809	0.885465
38	1	0	-7.478520	-1.802046	1.299728
39	1	0	-8.789537	-0.621698	1.277046
40	1	0	-7.302177	-0.278893	2.172109

41	1	0	-8.789549	-0.621672	-1.277022
42	1	0	-7.302194	-0.278864	-2.172092
43	1	0	-7.478539	-1.802027	-1.299729
44	1	0	7.184379	-1.947817	-0.885428
45	1	0	8.633012	-1.480086	0.000021
46	1	0	7.184366	-1.947816	0.885450
47	1	0	7.478522	1.802038	1.299738
48	1	0	8.789538	0.621688	1.277050
49	1	0	7.302176	0.278881	2.172111
50	1	0	8.789549	0.621682	-1.277018
51	1	0	7.302195	0.278876	-2.172091
52	1	0	7.478537	1.802035	-1.299720
53	1	0	-3.280362	-2.760760	0.000009
54	1	0	-5.677473	-2.386965	0.000014
55	1	0	-5.090070	1.879895	-0.000003
56	1	0	3.280362	2.760760	0.000010
57	1	0	5.677473	2.386965	0.000015
58	1	0	5.090069	-1.879895	-0.000003
59	1	0	3.046037	-3.646722	-0.000012
60	1	0	0.821002	-4.718901	-0.000017
61	1	0	-1.241468	-3.401056	-0.000016
62	1	0	1.241468	3.401056	-0.000016
63	1	0	-3.046037	3.646722	-0.000012
64	1	0	-0.821002	4.718901	-0.000017

---

tRc dimer (The dimer was constructed from geometrically optimized monomers placed at their crystallographic coordinates.)

C	4.943647	2.952091	-0.788426
C	6.297222	3.020879	-0.496639
H	6.741323	2.271878	0.153998
C	7.097823	4.049775	-1.034854
C	6.475405	4.990184	-1.868350
H	7.057362	5.795810	-2.301369
C	5.108392	4.934255	-2.172608
H	4.685495	5.692184	-2.824492
C	4.324268	3.916710	-1.638191
C	2.895708	3.575988	-1.753183
C	2.689212	2.416111	-0.971409
C	3.910138	1.995548	-0.361325
C	3.911341	0.879876	0.440862
H	4.817798	0.524716	0.924615
C	2.687543	0.174138	0.639577

H	2.693755	-0.707669	1.274853
C	1.503381	0.571384	0.055608
H	0.601102	-0.001337	0.239705
C	1.456716	1.726438	-0.786296
C	8.598352	4.101851	-0.693779
C	8.774232	4.241575	0.837458
H	8.323474	3.403029	1.378568
H	8.307768	5.163613	1.202618
H	9.839385	4.272278	1.098158
C	9.314543	5.288091	-1.366863
H	10.375885	5.280622	-1.094037
H	8.898704	6.250514	-1.047677
H	9.254537	5.234253	-2.459825
C	9.280802	2.797012	-1.169969
H	9.179771	2.675610	-2.254476
H	8.846912	1.911618	-0.693576
H	10.350511	2.815262	-0.927429
C	-1.701217	2.903713	-2.428544
C	-3.054792	2.834926	-2.720332
H	-3.498893	3.583928	-3.370970
C	-3.855394	1.806031	-2.182117
C	-3.232977	0.865621	-1.348621
H	-3.814934	0.059995	-0.915603
C	-1.865964	0.921549	-1.044363
H	-1.443067	0.163620	-0.392478
C	-1.081838	1.939094	-1.578779
C	0.346722	2.279816	-1.463787
C	0.553219	3.439693	-2.245561
C	-0.667707	3.860257	-2.855646
C	-0.668910	4.975928	-3.657832
H	-1.575367	5.331089	-4.141586
C	0.554889	5.681666	-3.856547
H	0.548677	6.563473	-4.491823
C	1.739050	5.284420	-3.272578
H	2.641330	5.857141	-3.456674
C	1.785715	4.129365	-2.430674
C	-5.355923	1.753955	-2.523193
C	-5.531802	1.614231	-4.054430
H	-5.081043	2.452777	-4.595540
H	-5.065339	0.692193	-4.419590
H	-6.596956	1.583528	-4.315130
C	-6.072114	0.567715	-1.850109
H	-7.133456	0.575185	-2.122936
H	-5.656276	-0.394707	-2.169295
H	-6.012109	0.621553	-0.757148
C	-6.038372	3.058794	-2.047003
H	-5.937341	3.180196	-0.962496
H	-5.604481	3.944188	-2.523395
H	-7.108081	3.040545	-2.289543

C	4.186198	-3.236179	-0.733031
C	5.539773	-3.167391	-0.441244
H	5.983874	-3.916392	0.209394
C	6.340374	-2.138495	-0.979459
C	5.717956	-1.198086	-1.812955
H	6.299913	-0.392460	-2.245974
C	4.350943	-1.254015	-2.117213
H	3.928046	-0.496086	-2.769097
C	3.566819	-2.271560	-1.582796
C	2.138259	-2.612282	-1.697788
C	1.931763	-3.772159	-0.916014
C	3.152688	-4.192722	-0.305930
C	3.153892	-5.308394	0.496257
H	4.060349	-5.663554	0.980010
C	1.930094	-6.014132	0.694972
H	1.936306	-6.895939	1.330248
C	0.745932	-5.616886	0.111003
H	-0.156347	-6.189607	0.295100
C	0.699267	-4.461832	-0.730901
C	7.840903	-2.086419	-0.638384
C	8.016783	-1.946695	0.892853
H	7.566025	-2.785241	1.433964
H	7.550319	-1.024657	1.258013
H	9.081936	-1.915992	1.153553
C	8.557094	-0.900179	-1.311468
H	9.618436	-0.907648	-1.038642
H	8.141255	0.062244	-0.992282
H	8.497088	-0.954017	-2.404429
C	8.523353	-3.391258	-1.114574
H	8.422322	-3.512660	-2.199081
H	8.089463	-4.276652	-0.638181
H	9.593062	-3.373008	-0.872034
C	-2.458666	-3.284557	-2.373149
C	-3.812241	-3.353344	-2.664937
H	-4.256342	-2.604342	-3.315574
C	-4.612843	-4.382239	-2.126722
C	-3.990426	-5.322649	-1.293226
H	-4.572383	-6.128275	-0.860208
C	-2.623413	-5.266721	-0.988967
H	-2.200516	-6.024650	-0.337083
C	-1.839287	-4.249176	-1.523384
C	-0.410727	-3.908454	-1.408392
C	-0.204230	-2.748577	-2.190166
C	-1.425156	-2.328013	-2.800250
C	-1.426359	-1.212342	-3.602437
H	-2.332816	-0.857181	-4.086190
C	-0.202560	-0.506604	-3.801152
H	-0.208772	0.375203	-4.436428
C	0.981601	-0.903851	-3.217182

H	1.883881	-0.331130	-3.401279
C	1.028266	-2.058905	-2.375279
C	-6.113372	-4.434315	-2.467798
C	-6.289251	-4.574039	-3.999035
H	-5.838492	-3.735493	-4.540145
H	-5.822788	-5.496077	-4.364195
H	-7.354405	-4.604742	-4.259735
C	-6.829563	-5.620555	-1.794714
H	-7.890905	-5.613085	-2.067541
H	-6.413725	-6.582978	-2.113900
H	-6.769558	-5.566717	-0.701752
C	-6.795821	-3.129476	-1.991608
H	-6.694790	-3.008074	-0.907101
H	-6.361930	-2.244082	-2.468000
H	-7.865530	-3.147725	-2.234148